Dynamic Power Conditioning Method of Microgrid Via Adaptive Inverse Control

Peng Li, *Senior Member, IEEE*, Xubin Wang, Wei-Jen Lee, *Fellow, IEEE*, and Duo Xu

***Abstract*—Different microsources have different frequency regulation functions and capabilities. The droop control can allocate power among the microsources according to the operation demand during system dynamics; however, the steady-state frequency often deviates from the rated value because of the droop characteristics. To ensure the precise condition of power and the stability of frequency even in a low-voltage network, this paper puts forward an improved droop control algorithm based on coordinate rotational transformation. With the ability to accurately regulate the unbalance power, this method realizes self-discipline parallel operation of microsources. Furthermore, an adaptive inverse control strategy applied to modified power conditioning is developed. With an online adjustment of modified $P-f$ droop coefficient for the frequency of microgrid to track the rated frequency, the strategy guarantees maintaining the frequency of microgrid at the rated value and meeting the important customers' frequency requirements. The simulation results from a multibus microgrid show the validity and feasibility of the proposed control scheme.**

***Index Terms*—Adaptive inverse control, dynamic power conditioning, microgrid, microsources, zero-error frequency regulation.**

I. Introduction

MICROGRID technology has provided a new technical approach for the large-scale integration of renewable energy and distributed generation [1], [2]. As a key building block of smart grid, microgrid has the potential to improve the utilization efficiency of energy cascade and improve power-supply reliability and power quality (PQ). Though microgrid has a flexible operation style, how to effectively control a variety of microsources in microgrid to ensure its safety, efficiency, and reliability in different operating modes are subjects of concern [3]–[5]. When the main grid fails to meet the PQ demand for the internal load in the microgrid, the microgrid will promptly disconnect from the main grid and operate in an autonomous mode. However, inertia of the microgrid is small when operating independently. Besides, there are other factors, such as nonlinear load and the randomness, volatility, and intermittent of microsources. As a result, it is difficult to control the system frequency and voltage accurately in the microgrid [6]–[8].

Peer-to-peer control is one of the hotspots of microgrid research. The primary objective of the peer-to-peer control of the microgrid is to assign power and distribute load among distributed generators without communication, for reducing the cost of microgrid, and enhancing the reliability and flexibility. In addition, a game-theoretic approach is presented to the control decision process of individual sources and loads in small-scale and dc power systems, and this game-theoretic methodology enhances the reliability and robustness of the microgrid by avoiding the need for central or supervisory control [9]. Game-theoretic communication helps to share local controller information, such as control input, individual objectives among controllers, and find a better optimized cost for the individual objectives [10]. For the robustness of the system operation, the peer to peer should be equipped with the feature of plug-n-play and hot swapping [11]–[14]. The conventional power droop control is suitable for the line parameters whose reactance is much larger than the resistance. But the resistance and reactance have the same order of magnitude in microgrids, and the conventional droop control is no longer applicable. So a new droop control strategy is needed [15]–[17]. To ensure the power quality (PQ), system frequency should be maintained within the desired range. Since most microsources are connected to microgrid through inverters, fixed droop coefficients will cause deviation between microgrid stable frequency and the rated value when output power is balanced [7], [14], [18]. There is a need to develop a new power control strategy combined with zero-error frequency regulation to mimic the primary and secondary frequency control of traditional power systems, which has the advantage of droop control and guarantees microgrid steady-state frequency maintained at the rated value.

After analyzing conventional droop control for the parallel-connected microsources, this paper introduces flat rotation transformation, an improved droop control and droop coefficient selection method, to enhance the operation of an LV microgrid. In addition, this paper proposes a novel power conditioning method based on adaptive inverse control to mitigate frequency deviation caused by the use of fixed $P-f$ droop coefficient [19], [20]. The proposed control method can dynamically and effectively balance power in the microgrid

Manuscript received November 30, 2013; revised March 03, 2014; accepted May 08, 2014. Date of publication January 14, 2015; date of current version March 20, 2015. This work was supported in part by the National Natural Science Foundation of China (50977029) and in part by the National High Technology Research and Development Program of China (863 Program) (2015AA050104). Paper no. TPWRD-01343-2013.

P. Li is with the State Key Laboratory of Alternate Electrical Power System with Renewable Energy Sources, North China Electric Power University, Baoding 071003, Hebei, China (e-mail: ncepulp@gmail.com).

X. Wang and D. Xu are with the School of Electrical and Electronic Engineering, North China Electric Power University, Baoding 071003, Hebei, China (e-mail: wbin.great@gmail.com; ncepuxd@gmail.com).

W. J. Lee is with the Energy Systems Research Center, University of Texas at Arlington, Arlington, TX 76019 USA (e-mail: wlee@uta.edu).

Color versions of one or more of the figures in this paper are available online at http://ieeexplore.ieee.org.

Digital Object Identifier 10.1109/TPWRD.2014.2323083

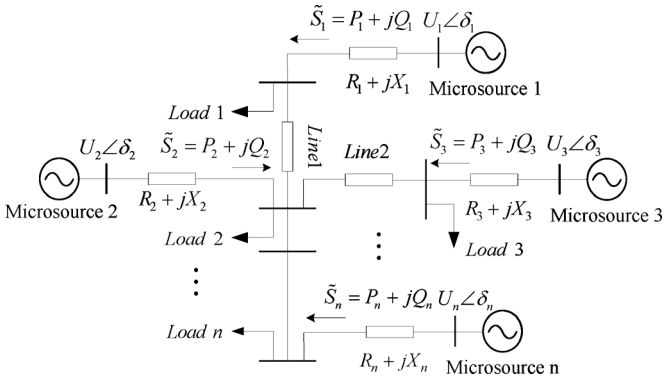

Fig. 1. Parallel operation system of microsources for autonomous microgrid.

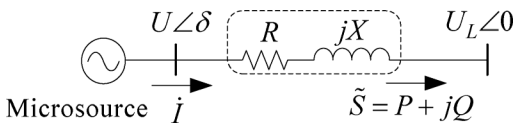

Fig. 2. Equivalent circuit of a parallel operation microsources.

while maintaining frequency at the rated value. The validity and feasibility of the proposed model are proved by simulation results.

II. Analysis of the Power Droop Control Method for the Microgrid

Fig. 1 depicts a parallel operation system of microsources for autonomous microgrid. Fig. 2 depicts the equivalent circuit of a microsources derived from Thevenin's theorem. According to the line power flow equation, output power of each microsource can be expressed as

$$\begin{aligned}\tilde{S} = P + jQ = \dot{U}\dot{I}^* &= \dot{U}\left(\frac{\dot{U} - \dot{U}_L}{R + jX}\right)^* \\ &= (U\cos\delta + jU\sin\delta)\left(\frac{U\cos\delta + jU\sin\delta - U_L}{R + jX}\right)^*\end{aligned} \tag{1}$$

where $\tilde{S}$ is the apparent power of microsources; P, Q are, respectively, the output active and reactive power of microsources; U is the voltage of microsources; δ is the phase angle of microsources output voltage; U_L is the load voltage; the phase angle of load voltage is zero; and R, X are, respectively, the line resistance and reactance.

Since the electrical distances between the sources and loads are short, it is reasonable to assume that the angle differences between the microsources and the load are very small. One can rewrite (1) by assuming $\cos\delta \approx 1, \sin\delta \approx \delta$

$$\begin{cases}\delta = \dfrac{XP - RQ}{UU_L} \\ \Delta U = U - U_L = \dfrac{RP + XQ}{U}\end{cases}. \tag{2}$$

A. Conventional Droop Control

For high-voltage (HV) lines, the reactance is much larger than the resistance $X \gg R$, and R can be ignored, according to (2), thus

$$\begin{cases}\delta = \dfrac{XP}{UU_L} \\ \Delta U = U - U_L = \dfrac{XQ}{U}\end{cases}. \tag{3}$$

For HV lines, the phase-angle deviation largely depends on active power, and the deviation of voltage magnitude largely depends on reactive power. In consideration of this, the microsources' output voltage can be directly controlled. Its phase angle can also be controlled by adjusting the output frequency, and the power sharing can be achieved by using droop control (4) for HV lines

$$\begin{cases}f = f_0 - kP \\ U = U_0 - mQ\end{cases} \tag{4}$$

where f_0 and U_0 are the no-load frequency and voltage, and k and m are the coefficients of conventional $P - f$ and $Q - U$ control.

B. Droop Control for LV Microgrid

Since the resistance and reactance have the same order of magnitude in a LV microgrid, the resistance cannot be ignored. When conventional droop control is applied to the LV microgrid, the accuracy of power sharing will be affected, and the stability of microgrid is threatened [5]. Thus, it is essential to reconsider the droop control for the characteristics of LV microgrid.

Given the characteristics of LV microgrid, (2) can be written as

$$\begin{bmatrix}\delta \\ \Delta U\end{bmatrix} = \begin{bmatrix}\frac{X}{UU_L} & -\frac{R}{UU_L} \\ \frac{R}{U} & \frac{X}{U}\end{bmatrix}\begin{bmatrix}P \\ Q\end{bmatrix}. \tag{5}$$

Since the resistance and reactance cannot be ignored, the regulation of frequency and voltage is coupled together with active power and reactive power. So a Givens transformation (flat rotation transformation) [21] is introduced in this paper, where flat rotation orthogonal matrix $\mathbf{J} = \begin{bmatrix}\sin\varphi & \cos\varphi \\ -\cos\varphi & \sin\varphi\end{bmatrix}$, φ is the phase angle of the line impedance, and Z is the line impedance. The schematic diagram of the Givens transformation is shown in Fig. 3, and (5) can be written as

$$\begin{aligned}\begin{bmatrix}\delta \\ \Delta U\end{bmatrix} &= \begin{bmatrix}\frac{X}{UU_L} & -\frac{R}{UU_L} \\ \frac{R}{U} & \frac{X}{U}\end{bmatrix}\mathbf{J}\mathbf{J}^{-1}\begin{bmatrix}P \\ Q\end{bmatrix} \\ &= \begin{bmatrix}\frac{Z}{UU_L} & 0 \\ 0 & \frac{Z}{U}\end{bmatrix}\begin{bmatrix}P' \\ Q'\end{bmatrix}\end{aligned} \tag{6}$$

where $\begin{bmatrix}P' \\ Q'\end{bmatrix} = \mathbf{J}^{-1}\begin{bmatrix}P \\ Q\end{bmatrix}$, defined as P' and Q', are modified active power and reactive power.

From Fig. 3 and (6), we can see that the phase-angle deviation δ only has a linear relationship with the modified active power and the deviation of voltage magnitude only has a linear relationship with the modified reactive power. Thus, accurate power sharing can be achieved by using a modified active power frequency $(P' - f)$ and modified reactive power voltage $(Q' - U)$

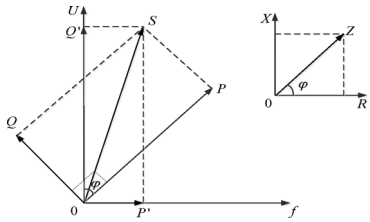

Fig. 3. Schematic diagram of the Givens transform.

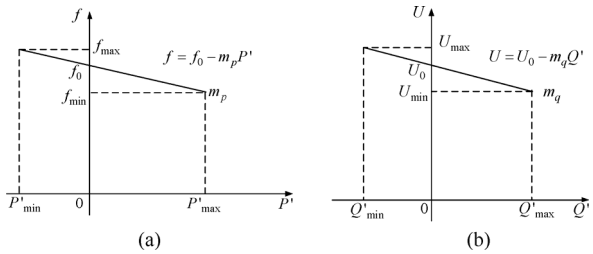

Fig. 4. Droop characteristic of the modified $P' - f$ and $Q' - U$. (a) $P' - f$ droop characteristics. (b) $Q' - U$ droop characteristics.

droop control strategy, which can be applied to the low-voltage (LV) microgrid.

$$\begin{cases} f = f_0 - m_p P' \\ U = U_0 - m_q Q' \end{cases} \tag{7}$$

where m_p and m_q are the coefficients of $P' - f$ and $Q' - U$ control.

Microsources output active power P and reactive power Q need to meet $0 \le P \le P_{\max}$ and $-Q_{\max} \le Q \le Q_{\max}$ in the conventional droop control. When using the modified active power frequency $(P' - f)$ and modified reactive power voltage $(Q' - U)$ droop control strategy, the modified active power P' and modified reactive power Q' should meet

$$P'_{\min} \le P' \le P'_{\max} \text{ and } Q'_{\min} \le Q' \le Q'_{\max}.$$

where $P'_{\min} = -(R)/(Z)Q_{\max}, P'_{\max} = (X)/(Z)P_{\max} + (R)/(Z)Q_{\max}, Q'_{\min} = -(X)/(Z)Q_{\max}$ and $Q'_{\max} = (R)/(Z)P_{\max} + (X)/(Z)Q_{\max}$. The characteristics of the modified active power frequency $(P' - f)$ and modified reactive power voltage $(Q' - U)$ droop control are shown in Fig. 4.

When using modified active power frequency $(P' - f)$ and modified reactive power voltage $(Q' - U)$ droop control strategies, all microsources with different power ratings should have the same no-load frequency and magnitude of no-load voltage, to ensure that no circulating current is produced between microsources at no-load operation. In order to meet relevant standards, the operating frequency should be maintained at between 49.5 and 50.5 Hz, and the voltage deviation should not exceed 5% of the rated value. Therefore, safe and stable operation of the microgrid can be guaranteed by selecting appropriate droop coefficients.

The modified active power frequency droop coefficient should meet the following three constraints:

1) no-load frequency of each microsource should be equal, so $f_{10} = f_{20} = \cdots = f_{i0} = \cdots = f_{n0} (i = 1, 2, \ldots, n)$;

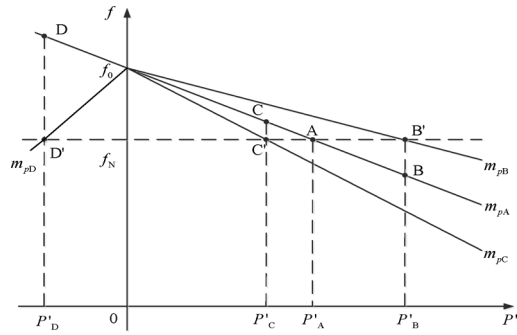

Fig. 5. Schematic diagram of the modified $P' - f$ droop control.

2) modified output active power of the microsources is $P'_{i\max}$, and its corresponding frequency should not be less than 49.5 Hz, so $f_{i\min} = f_{i0} - m_{\mathrm{ip}} P'_{i\max} \ge 49.5$;
3) modified output active power of the microsources is $P'_{i\min}$, and its corresponding frequency should not be higher than 50.5 Hz, so $f_{i\max} = f_{i0} - m_{\mathrm{ip}} P'_{i\min} \le 50.5$.

Similarly, modified reactive power frequency droop coefficients should meet the following three constraints:

1) no-load voltage of each microsource should be equal, so $U_{10} = U_{20} = \cdots = U_{i0} = \cdots = U_{n0} (i = 1, 2, \ldots, n)$;
2) modified output reactive power of the microsource is $Q'_{i\max}$, and its corresponding voltage should meet the equation $U_{i\min} = U_{i0} - m_{\mathrm{iq}} Q'_{i\max} \ge 0.95 U_{iN}$;
3) modified output reactive power of the microsource is $Q'_{i\min}$, and its corresponding voltage should meet the equation $U_{i\max} = U_{i0} - m_{\mathrm{iq}} Q'_{i\min} \le 1.05 U_{iN}$.

According to the aforementioned constraints, by selecting the appropriate modified active power frequency $(P' - f)$ and modified reactive power voltage $(Q' - U)$ droop coefficients, the unbalance power can be accurately regulated and the frequency and voltage can meet relevant PQ standards when the microgrid operates in an islanded mode.

III. Zero-Error Frequency Regulation Mechanism of Modified Active Power Frequency Droop Control

According to the analysis in the previous section, the characteristics of modified active power frequency droop can be obtained, and it can be concluded that modified active power should meet the equation $P'_{\min} \le P' \le P'_{\max}$. The adjusting process of the modified active power frequency droop control is shown in Fig. 5. Assuming that the initial steady-state operating point is A, at this time, the microsource operates at the rated value f_N, the output active power will be P_A, and the $P' - f$ slope coefficient will be m_{pA}. The following three cases are considered as follows.

1) When the load demand increases and the output modified active power will move to $P'_B (P'_{\min} \le P'_B \le P'_{\max})$, if droop coefficient m_{pA} is selected by conventional droop control, the operating point will move to B, and the output frequency will be less than f_N. If the droop coefficient is adjusted to m_{pB}, the operating point will be converted to B'; consequently, the frequency will return to f_N.
2) When the load demand decreases and the output modified active power will reduce to $P'_C (0 \le P'_C \le P'_A)$, if droop

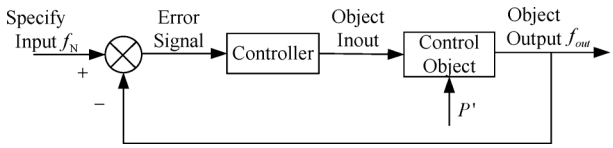

Fig. 6. Block diagram of modified $P' - f$ control with a feedback link.

coefficient m_{pA} is selected by conventional droop control, the operating point will move to C, and the output frequency will be higher than f_N. If the droop coefficient is adjusted to m_{pC}, the operating point will be converted to C'; consequently, the frequency will return to f_N.

3) When the load demand changes and the output modified active power will reduce to $P'_D(P'_{\min} \le P'_D \le 0)$, if droop coefficient m_{pA} is selected by using conventional droop control, the operating point will move to D, and the output frequency will be higher than f_N. If the droop coefficient is adjusted to m_{pD}, the operating point will be converted to D'; consequently, the frequency will return to f_N.

When the output modified active power increases or reduces to a new operating point due to the load demand changes and if the droop coefficient is selected by conventional droop control, the output frequency will be higher or less than f_N, even if it cannot meet relevant PQ standards. Thus, the advanced control method should be exploited to select the appropriate modified droop coefficients and reduce frequency deviation caused by load demand changes. Moreover, zero-error frequency regulation can be achieved, and frequency quality can be guaranteed. From the perspective of cybernetics, if the rated value f_N is regarded as the specified input and the output modified active power of microsources is regarded as the parameter of the controlled object, the controlled object is hoped to be controlled; in other words, the output frequency of the modified active power frequency droop control module can track the designated input. The control system diagram is shown in Fig. 6.

But in the microgrid, power fluctuations exist and output power of the microsources always changes. As a result, the mathematical model of the controlled object is in irregular dynamic change and cannot be established accurately in real time. As shown in Fig. 6, the conventional feedback cannot eliminate the system deviation caused by unbalance power. So a control algorithm is needed to follow the rated frequency with a real-time adjusting controller. This paper proposes a power conditioning method based on adaptive inverse control for the microgrid, which covers primary and secondary frequency control of the traditional control algorithm. According to the load demand change, this method can adjust the parameters of the controller in real time to dynamically correct modified active power frequency droop coefficients, so that the active power frequency dynamic regulation can be achieved.

IV. Active Frequency Regulation Principle of Adaptive Inverse Control

Adaptive inverse control was first proposed in 1986 by Professor B. Widrow at Stanford University [20]. It is an adaptive algorithm based on control method. The basic idea is that using a signal from the controller to drive the object, and the transfer

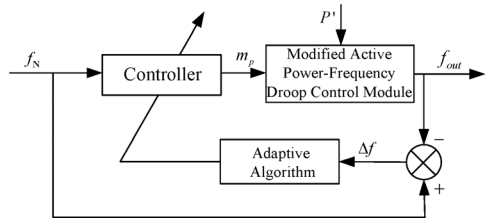

Fig. 7. Principle diagram of $P' - f$ droop control based on adaptive inverse control.

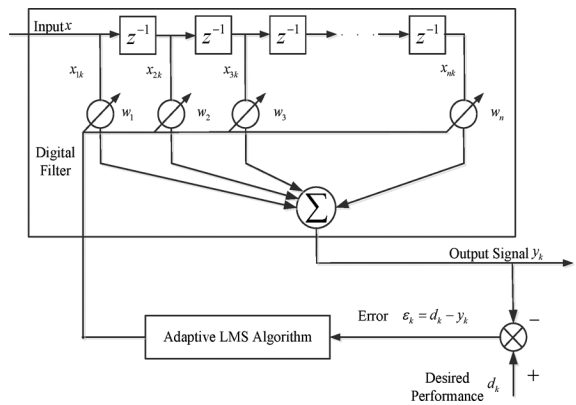

Fig. 8. Principle diagram of the adaptive LMS filter.

function of the controller is the inverse of the transfer function of the object itself. The controller generally has a finite impulse response (Finite Impulse Response, FIR) structure. Generally the object is either unknown or in a dynamic changing, real-time adjustment of the parameters of the controller is required to create the inverse [19]. For a microgrid modified active power frequency droop control module, the control schematic shown in Fig. 7 can be established using adaptive inverse control method.

In Fig. 7, the rated frequency f_{N} is the command input; modified active power frequency droop coefficient m_p can be used as a drive signal; the modified active power frequency droop control module is the object of adaptive inverse control, the module contains a non-linear variable, and that is modified active power P'. As can be seen, the key of an adaptive inverse control method is to find an adaptive algorithm for the controller parameters adjustment, to make the transfer function of the controller approach to the inverse function of the controlled object stably and fast.

At present, many adaptive algorithms can be used to automatically adjust weight coefficients of the controller such as differential steepest descent (DSD) algorithm, linear stochastic search (LRS) method, adaptive LMS (Least Mean Square) algorithm and so on. Among them, the adaptive LMS algorithm is widely used because of its fast convergence speed and good stability, etc. The gradient descent method is used in the adaptive LMS algorithm to adjust weight coefficients of the controller online. LMS filter are composed of adaptive LMS algorithm and digital filters with FIR digital structure. It is applied in adaptive inverse control system.

The adaptive LMS filter schematic is shown in Fig. 8:

Let the kth input signal vector be

$$\mathbf{X}_k = [x_{1k}, x_{2k}, x_{3k} \ldots, x_{nk}]^{\mathrm{T}}. \tag{8}$$

Let the weight coefficient vector be

$$\mathbf{W}^{\mathrm{T}} = [w_1, w_2, w_3 \ldots, w_n]^{\mathrm{T}}. \tag{9}$$

And then the kth output signal vector is

$$y_k = \sum_{i=0}^{n} w_i x_{ik} = \mathbf{W}^{\mathrm{T}}\mathbf{X}_k = \mathbf{X}_k^{\mathrm{T}}\mathbf{W}. \tag{10}$$

Define the error between the output signal and the expected response d_k as

$$\varepsilon_k = d_k - y_k = d_k - \mathbf{W}^{\mathrm{T}}\mathbf{X}_k = d_k - \mathbf{X}_k^{\mathrm{T}}\mathbf{W}. \tag{11}$$

Find the mean square error (MSE)

$$\begin{aligned}\mathrm{MSE} &= E\left[\varepsilon_k^2\right] = E\left[d_k^2\right] - 2E\left[d_k\mathbf{X}_k^{\mathrm{T}}\right]\mathbf{W} + \mathbf{W}^{\mathrm{T}}E\left[\mathbf{X}_k\mathbf{X}_k^{\mathrm{T}}\right]\mathbf{W} \\ &= E\left[d_k^2\right] - 2\mathbf{R}_{xd}^{\mathrm{T}}\mathbf{W} + \mathbf{W}^{\mathrm{T}}\mathbf{R}_{xx}\mathbf{W}. \end{aligned}\tag{12}$$

Define the cross-correlation vector of the input signal and the expected response $\mathbf{R}_{xd}$ as

$$\mathbf{R}_{xd} = E[d_k\mathbf{X}_k] = E\begin{bmatrix} d_k x_{1k} \\ d_k x_{2k} \\ \cdots \\ d_k x_{\mathrm{nk}} \end{bmatrix}. \tag{13}$$

The autocorrelation matrix of input signal symmetric and positive definite (or semi-definite) input $\mathbf{R}_{xx}$ is

$$\mathbf{R}_{xx} = E[\mathbf{X}_k\mathbf{X}_k^{\mathbf{T}}] = E\begin{bmatrix} x_{1k}x_{1k} & x_{1k}x_{2k} & \cdots \\ x_{2k}x_{1k} & x_{2k}x_{2k} & \cdots \\ \cdots & \cdots & x_{nk}x_{nk} \end{bmatrix}. \tag{14}$$

It can be seen from (12), that the mean square error is a quadratic function about the weight coefficient vector. It is an intermediate upwardly convex parabolic surface and has a unique minimum. Adaptive process will continuously adjust these weight coefficients to make the mean square error minimum, which is equivalent to down along a parabolic shape surface to find the minimum.

By differentiating MSE function with respect to the weight coefficient vector in (12), the gradient vector of the mean square error function can be written as

$$\begin{aligned}\nabla_{(k)} &= \left[\frac{\partial E\left[\varepsilon_k^2\right]}{\partial w_1}, \frac{\partial E\left[\varepsilon_k^2\right]}{\partial w_2}, \ldots, \frac{\partial E\left[\varepsilon_k^2\right]}{\partial w_n}\right]^{\mathrm{T}} \\ &= -2\mathbf{R}_{xd} + 2\mathbf{R}_{xx}\mathbf{W}. \end{aligned}\tag{15}$$

Taking ε_k^2 as an estimation value of the mean square error, $E[\varepsilon_k^2]$, ∇_k can be expressed as

$$\hat{\nabla}_k = \nabla\left[\varepsilon_k^2\right] = 2\varepsilon_k\nabla[\varepsilon_k] \tag{16}$$

where $\nabla[\varepsilon_k] = \nabla[d_k - \boldsymbol{W}_k^{\mathbf{T}}\boldsymbol{X}_k] = -\boldsymbol{X}_k$, and create iterative formula of the weight coefficient vector according to $\hat{\nabla}_k$:

$$\mathbf{W}_{k+1} = \mathbf{W}_k + 2\mu\varepsilon_k\mathbf{X}_k \tag{17}$$

where μ is a constant used for controlling convergence speed and stability called convergence factor.

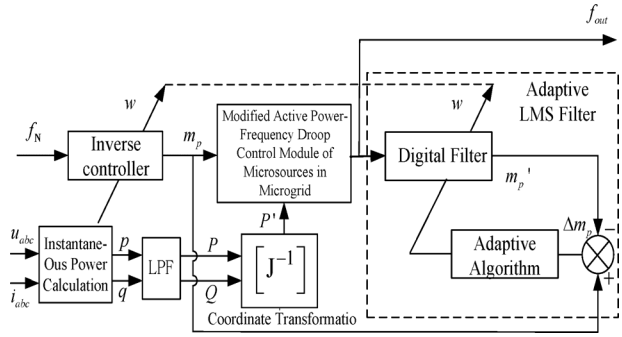

Fig. 9. Principle diagram of active power conditioning based on adaptive inverse control.

V. Active Power Conditioning Based on Adaptive Inverse Control

Fig. 9 shows that the modified active power frequency adjustment method of the microgrid via adaptive inverse control includes an instantaneous power calculation unit, coordinate rotation transformation unit, and adaptive inverse control unit.

In the instantaneous power calculation unit, instantaneous active power p and instantaneous reactive power q are obtained by the three-phase voltage u_{abc} and current i_{abc} of the output of microsources through instantaneous power calculation, and then the active power P and reactive power Q is obtained through a low-pass filter; in the coordinate rotation transformation unit, the active power P is transformed into the modified active power P'; the adaptive inverse control unit consists of inverse controller, modified active power frequency droop control module of microsources and adaptive LMS filters. The error of the adaptive inverse control unit is aimed at the error of the object output. But according to the adaptive LMS algorithm the error of LMS adaptive filter is aimed at the object input, so this algorithm cannot be directly applied to the adaptive inverse control basic mode shown in Fig. 7. In order to implement the adaptive LMS algorithm, and obtain a proper error, the corresponding adaptive inverse control unit shown in Fig. 8 is developed as the equivalence to the basic model shown in Fig. 7.

The pre-posed inverse controller can be seen as an equivalent copy of the digital filter with identical structure and coefficients. Modified active power frequency droop coefficient m_p is obtained by the weighted sum of command input f_{N} through the inverse of the controller; thus according to m_p and the current modified active power of microsources, the modified active power frequency droop control module can obtain the current frequency f_{out}; furthermore, modified active power frequency droop coefficient m_p' corresponding to reference frequency is obtained by delivering f_{out} into the digital filter; finally according to the error of m_p and m_p', the adaptive algorithm adjusts the weight coefficients of the digital filter and the pre-posed inverse controller online, so that the optimal values of the modified active power frequency droop coefficients can be found along the direction of the negative gradient of the mean square error. When the error of m_p and m_p' is zero, the modified active power frequency droop control module outputs frequency f_{out} to track the rated frequency f_{N}. At this moment the inverse

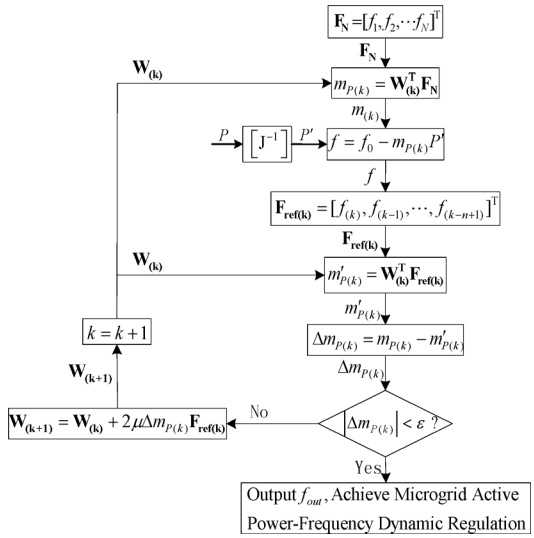

Fig. 10. Algorithm flowchart of the active power conditioning method based on adaptive inverse control.

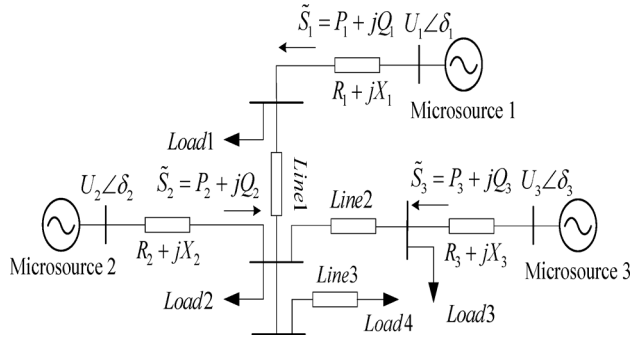

Fig. 11. Network topology diagram of a microgrid.

controller is exactly the inverse function of the modified active power frequency droop control module. Mimicking the primary and secondary frequency control of traditional power systems, zero-error frequency regulation is achieved through the adaptive inverse control system in microgrid. The flowchart of the active power frequency adjustment based on the adaptive LMS algorithm is shown in Fig. 10.

In adaptive LMS algorithm the convergence speed and stability is related to the selection of initial values of weight coefficients and convergence factors. In order to ensure stable operation at the initial moment, initial values of the modified active power frequency droop coefficients should be selected according to the relevant power quality standards as described in Section 1. The initial values of weight coefficients can be obtained by the following formula:

$$w_{(0)} = \frac{m_{p(0)}}{(n+1)f_{\mathrm{N}}}. \tag{18}$$

And the selection of convergence factor μ is in accordance with the principles of the steepest descent algorithm. Let $\lambda_i i = 1, 2, 3, \ldots, n+1$ be the first characteristic value of $\mathbf{R}_{xx}$, as shown in (19), at the bottom of the page.

Ensure the convergence of iterative calculation and let $\lambda_{\max} = \max(\lambda_1, \lambda_2, \ldots, \lambda_{n+1})$ and μ meet the constraint $0 < \mu < (1)/(\lambda_{\max})$.

VI. Simulated Results

A microsource-interconnected and independent microgrid system shown in Fig. 11, based on the Matlab/Simulink platform, is developed to verify the correctness and feasibility of the proposed dynamic power conditioning method of the microgrid via adaptive inverse control.

As is seen in Fig. 11, the microgrid contains three microsources and three loads. Network parameters: $R_1 = R_3 = 0.1\ \Omega, R_2 = 0.15\ \Omega, X_1 = X_2 = 0.2\ \Omega, X_3 = 0.15\ \Omega$; the line type of Line1, Line2, and Line3 are, respectively, LJ-16 (0.5 km), LJ-50 (0.3 km) and LJ-35 (0.1 km); the active and reactive power of Load1, 2, 3 and 4 are set at 2.5 kW and 1.55 kVar. The active and reactive power of load 3 increase to 15 kW and 9.3 kVar at $t = 0.5$s and the microsource 2 is turned on at $t = 1.0$s. The active power frequency droop coefficient initial values of microsource 1, 2, and 3 are, respectively, $1.978 \times 10^{-4}, 2.108 \times 10^{-4}$ and 2.108×10^{-4}. The convergence factor μ of adaptive inverse control is set at 3.14×10^{-5}.

As is seen in Fig. 12(a), when using conventional droop control method, the output power distribution is unreasonable. When putting microsource 2 on at $t = 1.0$ s, the output active power P_1, P_2 and P_3 of microsources has a large transient dynamic response, in other words, the dynamic response characteristic is bad. Fig. 12(b) shows that output reactive power Q_1 and Q_3 are negative and microsources begin to absorb the reactive power, so the reactive circulating-current occurs when microsource 2 is connected to the microgrid. As is seen in Fig. 12(c), the system frequency fluctuates badly because of the sudden load increases at $t = 0.5$ s and the access of microsource 2 at $t = 1.0$ s. And the fluctuation quantity in the transient process exceeds the quality standards. According to Fig. 12(a) and (b), total output active and reactive power are close to 26 kW and 15 kVar, and total active and reactive loads are 22.5 kW and 13.95 kVar, respectively, during time period 0.5 s to 1.0 s. Therefore, total active power generation can support the total loads and network losses in the system. Fig. 13 is the frequency fluctuation curve of modified droop control. It shows that frequency droop control than the traditional method

$$\begin{aligned} |\mathbf{R}_{xx} - \lambda\mathbf{E}| &= \begin{vmatrix} f_{\mathrm{out}(k)}^2 - \lambda & f_{\mathrm{out}(k)}f_{\mathrm{out}(k-1)} & \cdots & f_{\mathrm{out}(k)}f_{\mathrm{out}(k-n)} \\ f_{\mathrm{out}(k-1)}f_{\mathrm{out}(k)} & f_{\mathrm{out}(k-1)}^2 - \lambda & \cdots & f_{\mathrm{out}(k-1)}f_{\mathrm{out}(k-n)} \\ \cdots & \cdots & \cdots & \cdots \\ f_{\mathrm{out}(k-n)}f_{\mathrm{out}(k)} & f_{\mathrm{out}(k-n)}f_{\mathrm{out}(k-1)} & \cdots & f_{\mathrm{out}(k-n)}^2 - \lambda \end{vmatrix} \\ &= (\lambda - \lambda_1)(\lambda - \lambda_2)\cdots(\lambda - \lambda_{n+1}) = 0. \end{aligned} \tag{19}$$

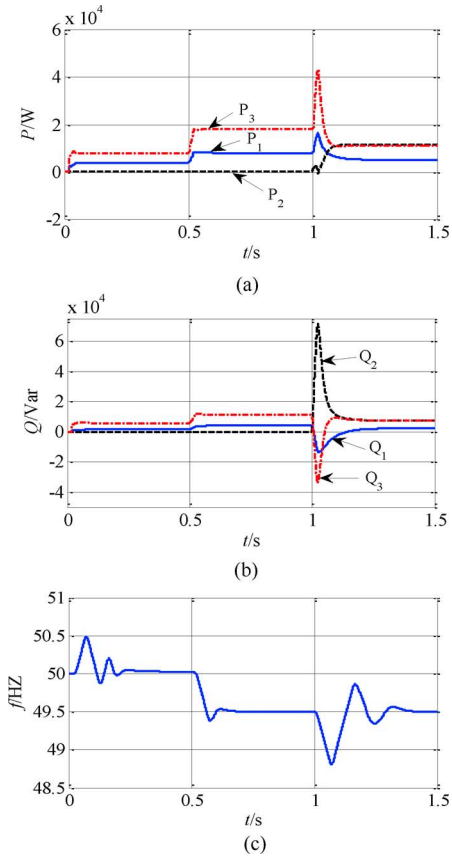

Fig. 12. Simulation curves of traditional droop control. (a) Active power output curves of conventional droop control method. (b) Reactive power output curves of the conventional droop control method. (c) Frequency variation curve of the conventional droop control method.

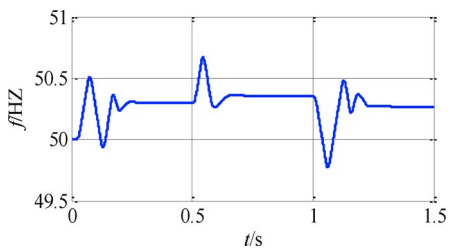

Fig. 13. Frequency fluctuation curve of the modified droop control.

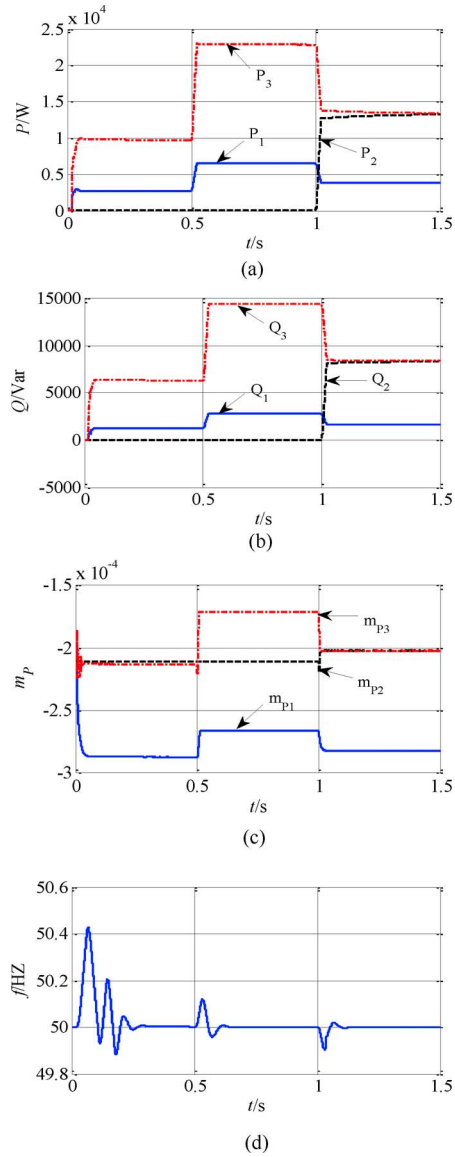

Fig. 14. Simulation curves of active power conditioning based on adaptive inverse control. (a) Active power output curves of adaptive inverse control. (b) Reactive power output curves of adaptive inverse control. (c) Active power frequency droop coefficient variation curves of adaptive inverse control. (d) Frequency variation curve of adaptive inverse control.

has some improvements. The microgrid frequency basically fluctuates above and below 50.3 Hz, but its transient fluctuation is not improved.

As can be seen in Fig. 14(a), when using active power conditioning based on adaptive inverse control, microsource can make a reasonable distribution of load according to the dynamic variation of active power frequency droop coefficients m_{P1}, m_{p2} and m_{p3}. And during the sudden load fluctuation of microsources and the access of microsource 2, the transition of output active power is smoother which is in accordance with the "plug and play" concept in peer-to-peer control of microgrid. Compared with Fig. 12(b), Fig. 14(b) shows that reactive circulating-current does not occur and its dynamic response characteristic is improved. According to Fig. 14(a) and (b), total output active and reactive power are close to 28 kW and 16 kVar during time period 0.5 s to 1.0 s, so total active power generation can support total loads and network losses in the system. Fig. 14(c) shows that active power frequency droop coefficients vary with the change of the microsources output active power (when $t \leq 1.0$ s microsource 2 is not put into operation, the droop coefficient m_{p2} remains at the initial value). Because of the use of adaptive LMS algorithm, the active power frequency droop coefficients have a fast convergence speed in the whole process of searching for optimal values. In Fig. 14(d), the system frequency stabilizes at the rated frequency 50 Hz after a short fluctuation with a narrow range during the sudden load fluctuation and the access of microsource 2.

VII. Conclusion

Conventional droop control has fixed droop coefficients; it will cause frequency deviation and so that it cannot guarantee

the output frequency will reach the steady-state index when applied to the microgrid. Due to the characteristics of the line parameters and the operating frequency regulation, this paper proposes a power conditioning method based on adaptive inverse control. Theoretical analysis and simulation results show that this method can dynamically adjust the weight coefficients of digital filters online and in real time, in order to achieve accurate power balance regulation and zero-error frequency regulation. The proposed method is suitable for the parallel operation system of microsources in an autonomous microgrid. Moreover, it provides a strong guarantee to the stable operation of the microgrid.

REFERENCES

[1] R. H. Lasseter, "Microgrids," in *Proc. IEEE Power Eng. Soc. Winter Meeting*, Jan. 2002, pp. 305–309.

[2] J. A. P. Lopes, C. L. Moreira, and A. G. Madureira, "Defining control strategies for microgrids islanded operation," *IEEE Trans. Power Syst.*, vol. 21, no. 2, pp. 916–924, May 2006.

[3] F. Katiraei and M. R. Iravani, "Power management strategies for a microgrid with multiple distributed generation units," *IEEE Trans. Power Syst.*, vol. 21, no. 4, pp. 1821–1831, Nov. 2006.

[4] M. H. J. Bollen and A. Sannino, "Voltage control with inverter-based distributed generation," *IEEE Trans. Power Del.*, vol. 20, no. 1, pp. 519–520, Jan. 2005.

[5] A. Engler and N. Soultanis, "Droop control in LV-grids," in *Proc. Int. Conf. Future Power Syst.*, Nov. 16–18, 2005, vol. 1, pp. 1–6.

[6] H. Karimi, H. Nikkhajoei, and M. R. Iravani, "Control of an electronically-coupled distributed resource unit subsequent to an islanding event," *IEEE Trans. Power Del.*, vol. 23, no. 1, pp. 493–501, Jan. 2008.

[7] F. Katiraei, M. R. Iravani, and P. W. Lehn, "Micro-grid autonomous operation during and subsequent to islanding process," *IEEE Trans. Power Del.*, vol. 20, no. 1, pp. 248–257, Jan. 2005.

[8] J. V. Milanovic, M. T. Aung, and S. C. Vegunta, "The influence of induction motors on voltage sag propagation—Part II: Accounting for the change in sag performance at LV buses," *IEEE Trans. Power Del.*, vol. 23, no. 2, pp. 1072–1078, Apr. 2008.

[9] W. W. Weaver and P. T. Krein, "Game-theoretic control of small-scale power systems," *IEEE Trans. Power Del.*, vol. 24, no. 3, pp. 1560–1567, Jul. 2009.

[10] N. C. Ekneligoda and W. W. Weaver, "Game-theoretic communication structures in microgrids," *IEEE Trans. Power Del.*, vol. 27, no. 4, pp. 2334–2341, Oct. 2012.

[11] M. B. Delghavi and A. Yazdani, "Islanded-mode control of electronically coupled distributed-resource units under unbalanced and nonlinear load conditions," *IEEE Trans. Power Del.*, vol. 26, no. 2, pp. 661–673, Apr. 2010.

[12] R. Majumder, B. Chaudhuri, A. Ghosh, R. Majumder, G. Ledwich, and F. Zare, "Improvement of stability and load sharing in an autonomous microgrid using supplementary droop control loop," *IEEE Trans. Power Syst.*, vol. 25, no. 2, pp. 796–808, May 2010.

[13] R. Majumder, G. Ledwich, A. Ghosh, S. Chakrabarti, and F. Zare, "Droop control of converter-interfaced microsources in rural distributed generation," *IEEE Trans. Power Del.*, vol. 25, no. 4, pp. 2768–2778, Oct. 2010.

[14] S. Chiniforoosh, J. Jatskevic, A. Yazdani, V. Sood, V. Dinavahi, J. A. Martinez, and A. Ramirez, "Definitions and applications of dynamic average models for analysis of power systems," *IEEE Trans. Power Del.*, vol. 25, no. 4, pp. 2655–2669, Oct. 2010.

[15] M. A. Zamani, T. S. Sidhu, and A. Yazdani, "A protection strategy and microprocessor-based relay for low-voltage microgrids," *IEEE Trans. Power Del.*, vol. 26, no. 3, pp. 1873–1883, Jul. 2011.

[16] P. Piagi and R. H. Lasseter, "Autonomous control of microgrids," in *Proc. IEEE Power Eng. Soc. Meeting*, Montactive, QC, Canada, Jun. 2006. [Online]. Available: http://certs.lbl.gov/CERTS_P_DER.html

[17] H. Karimi, E. J. Davison, and R. Iravani, "Multivariable servomechanism controller for autonomous operation of a distributed generation unit: Design and performance evaluation," *IEEE Trans. Power Syst.*, vol. 25, no. 2, pp. 853–865, May 2010.

[18] S. K. Parlak, M. Ozdemir, and T. Aydemir, "Active and reactive power sharing and frequency restoration in a distributed power system consisting of two UPS units," *Elect. Power Energy Syst.*, vol. 31, pp. 220–226, 2009.

[19] G. L. Plett, "Adaptive inverse control of linear and nonlinear systems using dynamic neural networks," *IEEE Trans. Neural Netw.*, vol. 14, no. 2, pp. 360–376, Mar. 2003.

[20] B. Widrow and E. Walach, *Adaptive Inverse Control*. Upper Saddle River, NJ, USA: Prentice-Hall, 1996.

[21] Gautschi and Walter, *Numerical Analysis*. New York, USA: Springer, 2011.

Peng Li (M'06–SM'11) received the B.S., M.S., and Ph.D. degrees in electrical engineering from the North China Electric Power University, Baoding, Hebei, China, in 1988, 1993, and 2004, respectively.

Currently, he is a Full Professor with the North China Electric Power University. His research interests include distributed generation, microgrid, power-quality analysis and control, and power-electronics technology applications in power systems.

Xubin Wang received the B.S. degree in electrical engineering from the North China Electric Power University, Baoding, Hebei, China, in 2012.

Currently, he is a Postgraduate of North China Electric Power University. His main research interests include distributed generation and microgrid technology.

Wei-Jen Lee (S'85–M'85–SM'97–F'07) received the B.S. and M.S. degrees in electrical engineering from National Taiwan University, Taipei, Taiwan, in 1978 and 1980, respectively, and the Ph.D. degree in electrical engineering from the University of Texas, Arlington, TX, USA, in 1985.

In 1985, he joined the University of Texas, Arlington, where he is currently a Professor of the Electrical Engineering Department and the Director of the Energy Systems Research Center. He has been involved in research on arc flash and electric safety, power flow, transient and dynamic stability, voltage stability, short circuits, relay coordination, power-quality analysis, renewable energy, and deregulation for utility companies.

Prof. Lee is a registered Professional Engineer in the State of Texas.

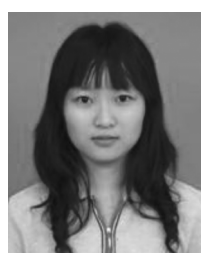

Duo Xu received the B.S. degree in electrical engineering from the North China Electric Power University, Baoding, Hebei, China, in 2013.

Currently, she is a Postgraduate from North China Electric Power University. Her main research interests include distributed generation and microgrid technology.